iScience

CellPress
OPEN ACCESS

Article

Smurf1 silencing restores PTEN expression that ameliorates progression of human glioblastoma and sensitizes tumor cells to mTORC1/C2 inhibitor Torin1

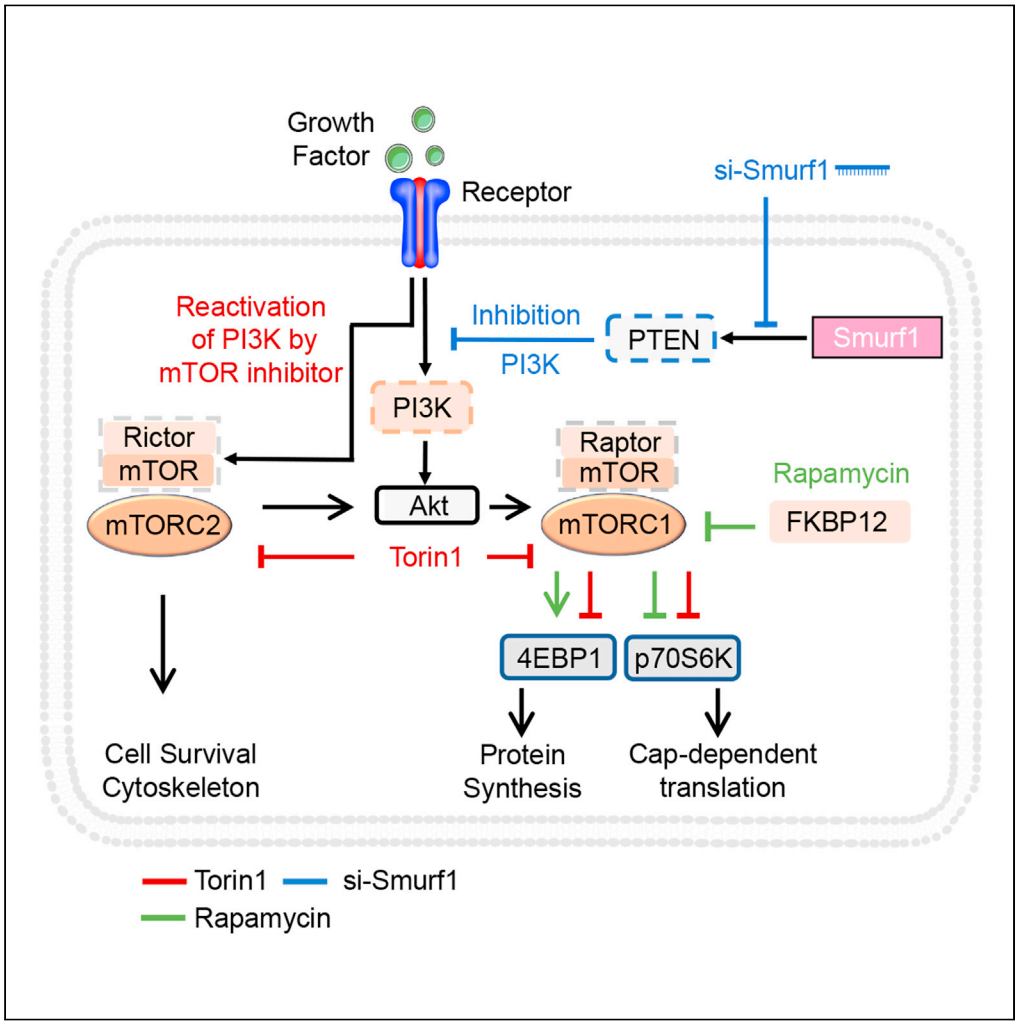

Qin Xia, Wenxuan Li, Sakhawat Ali, ..., Xinyi Meng, Liqun Liu, Lei Dong

ldong@bit.edu.cn

Highlights

Smurf1 ubiquitylates and degrades PTEN, leading to upregulating oncogenic pathways

Loss of Smurf1 resensitizes tumor cells to mTOR inhibitor Torin1 in PTEN-wild type GB

Smurf1 depletion with Torin1 has enhanced efficacy by inhibiting pho-4EBP1 and pho-S6K

Smurf1 suppression with Torin1 is toxic to Rapamycin resistant GB cells

Xia et al., iScience *24*, 103528
December 17, 2021 © 2021
https://doi.org/10.1016/j.isci.2021.103528

iScience

CellPress
OPEN ACCESS

Article

Smurf1 silencing restores PTEN expression that ameliorates progression of human glioblastoma and sensitizes tumor cells to mTORC1/C2 inhibitor Torin1

Qin Xia,[1] Wenxuan Li,[1] Sakhawat Ali,[1] Mengchuan Xu,[1] Yang Li,[1] Shengzhen Li,[1] Xinyi Meng,[1] Liqun Liu,[1] and Lei Dong[1,2,*]

SUMMARY

Amplification of ubiquitin E3 ligase Smurf1 promotes degradation of PTEN leading to hyperactivation of the Akt/mTORC1 pathway. However, inhibitors of this pathway have not hitherto yielded promising results in clinical studies because of strong drug resistance. Here, we investigated Smurf1 expression in various glioblastoma (GB) cell lines and patient tissues. The therapeutic efficacy of Smurf1 silencing and Torin1 treatment was assessed in GB cells and orthotopic mouse model. We found Smurf1 loss elevates PTEN levels that interrupt the epidermal growth factor receptor pathway activity. Cotreatment with Smurf1 silencing and mTORC1/C2 inhibitor Torin1 remarkably decreased phosphorylation of Akt, and mTORC1 downstream targets 4EBP1 and S6K resulting in synergistic inhibitory effects. Smurf1 knockdown in orthotopic GB mouse model impaired tumor growth and enhanced cytotoxicity of Torin1. Together, these findings suggest a rational combination of Smurf1 inhibition and Torin1 as a promising new avenue to circumvent PI3K/Akt pathway-driven tumor progression and drug resistance.

INTRODUCTION

Glioblastoma (GB) is the deadliest and most common primary brain tumor, with a median post diagnosis survival of 15 months (Furnari et al., 2007; Meyer, 2008). Radiotherapy is a standard procedure in GB treatment, and current treatment with temozolomide is beneficial in patients with hypermethylated MGMT promoter. Chemotherapeutic drugs play a critical adjuvant role in patients with GB after surgical treatment. The epidermal growth factor receptor (EGFR) and Phosphatase and tensin homolog (PTEN) gene mutations are commonly found in GB cells (Brennan et al., 2013; Cancer Genome Atlas Research, 2008; Li et al., 1997). EGFR is a tyrosine kinase (TK) receptor that regulates fundamental cell growth and proliferation. Overexpression of EGFR and its ligands, or gain of function mutation of EGFR, contributes to tumorigenesis and drug resistance (Paez et al., 2004; Yaish et al., 1988). Because of its crucial role in regulating cellular transformation and growth signals, EGFR has been focused on by multiple studies in GB. Akt is the main effector of EGFR downstream signaling, and phosphorylated-Akt (p-Akt) is the prime activation trigger of EGFR pathways (Moores et al., 2016).

PTEN gene encodes a cytoplasmic protein with both protein and lipid phosphatase activity (Yang et al., 2017). PTEN converts PIP3 to PIP2, and loss of PTEN function leads to phosphorylation of PI3K (p-PI3K) that triggers Akt overactivation, which is associated with poor prognosis of GB (Yang et al., 2010). Activated Akt is also associated with TK activation, a likely further GB cell survival strategy. Hence, PTEN is a crucial checkpoint in Akt signaling, and its dysfunction activates RTK-dependent carcinogenesis. Therefore, this line of evidence suggests TKs confer a therapeutic effect that appears encouraging and should be pursued. Recently, more attention has been focused on TK inhibitors as a treatment option against gliomas; however, clinical results did not show an appreciable increase in the survival of patients treated concurrently with TK inhibitors and chemoradiotherapy. More importantly, GB patients with different PTEN status also contribute to their prognosis and therapeutic strategy (Xie et al., 2021). Chen et al. reported that inhibition of YAP1-LOX-β1 integrin-PYK2 axis reduces macrophage infiltration and PTEN-null glioma growth (Chen et al., 2019).

[1]School of Life Science, Beijing Institute of Technology, Beijing 100081, China

[2]Lead contact

*Correspondence: ldong@bit.edu.cn

https://doi.org/10.1016/j.isci.2021.103528

Hyperactivated PI3K/Akt/mTOR pathway suppresses autophagy, promotes oncogenic growth, and confers resistance to many chemotherapy drugs (Cancer Genome Atlas Research, 2008; Zhao et al., 2017). Therefore, mTOR inhibitors combine with chemotherapy to alleviate resistance because of sustained activated PI3K/Akt/mTOR signaling. Several small molecule inhibitors of mTOR have been developed to treat GB, with different mechanisms of action. Torin1 is a second-generation, ATP-competitive inhibitor that inhibits both mTORC1 and mTORC2 (Melick and Jewell, 2020). Although it seems promising, broad side effects and the emergence of resistance have hampered the clinical success of mTOR inhibitors. Resistance against mTOR inhibitors can be correlated with the oncogene-driven overactivation of signaling pathways, such as PI3K/Akt/mTOR and MEK/ERK pathways. Smad ubiquitylation regulatory factor 1 (Smurf1) confers malignant phenotype to human cancer cells (Xie et al., 2014), but the molecular mechanism underlying Smurf1 activity in GB chemotherapy remains largely unexplored.

Recent data showed that Smurf1 expression increases in higher WHO Grade and is associated with a worse prognosis in glioma patients (Chang et al., 2018). Another report showed downregulation of Smurf1 in GB cells decreases PI3K/Akt pathway, leading to growth suppression, enhanced apoptosis, and cell-cycle arrest, which could theoretically enhance the chemotherapeutic effects of cancer therapy (Chang et al., 2018). Our previous study established Smurf1 as an important regulator of growth signaling in PTEN wild-type cells and thus represents a candidate accounting for drug resistance. Importantly, two main reasons account for clinical ineffectiveness, even drug resistance of rapamycin (allosteric inhibitor of mTORC1, but largely ineffective in inhibiting mTORC2 activity). First, rapamycin incompletely inhibits mTORC1 downstream 4EBP1 phosphorylation and is refractory to long-term rapamycin treatment, even though S6K phosphorylation remains permanently inhibited (Choo et al., 2008). Second, suppression of mTORC1 stimulates the negative-feedback loop of PI3K/Akt signaling and increases the survival of cancer cells.

Torin1 is a highly potent and selective mTORC1 (including sustained inhibition of 4EBP1 phosphorylation) and mTORC2 kinase inhibitor with strong biological activity in various preclinical settings (Thoreen et al., 2009). In this study, we sought to identify the impact of Smurf1 suppression on PI3K/Akt axis and Torin1 mediated chemotherapeutic effects in human PTEN mutant (U251, LNZ308, U87) and PTEN wild-type (LN229, U343) GB cells (Furnari et al., 1997; Ishii et al., 1999). We report that Smurf1 silencing antagonizes Akt/mTOR signaling, increases the sensitivity of Torin1 in GB cells and that inhibition of the mTORC1/4EBP1 axis is also essential for these effects. Suppression of Smurf1 synergistically enhanced Torin1 cytotoxicity in PTEN wild-type GB cells. Mechanistically, inhibition of Smurf1 combined with Torin1 treatment suppressed GB growth by elevating PTEN and by downregulating both Akt and S6K1 signaling. This study provides novel insights into the regulation of Akt/mTOR/S6K1 signaling cascade. Our data further demonstrate that Smurf1 plays a significant role in GB by regulating key signaling pathways where PTEN is active.

RESULTS

Smurf1 is elevated in GB patients and cell lines

Overexpression of Smurf1 is implicated in poor prognosis of glioma (Chang et al., 2018). Immunohistochemistry staining shows higher expression of Smurf1 protein in GB tissues (n = 5) compared to adjacent normal brain tissues (n = 3) (Figure 1A). Patient samples were also used to generate cell lines *in vitro* (primarily from patient #19005). Consistently, Smurf1 was expressed in all listed GB cell lines (Figure 1B). In general, the tested PTEN wild-type cell lines U343 and LN229 showed relatively decreased p-Akt than PTEN-mutant cells (LNZ308, U251, U87, U118, and #19005). Keeping in view the involvement of several E3 ubiquitin ligases in carcinogenesis, we started evaluating the impact of Smurf1 levels on GB progression and resistance to mTOR inhibitor Torin1.

Silencing of Smurf1 suppresses viability of GB cells

We hypothesized that high Smurf1 expression contributes to hijacked signaling pathways during tumor cell growth; therefore, we transfected GB cells with si-Smurf1 and si-Control. Smurf1 silencing significantly reduces p-Akt in PTEN wild-type GB cells LN229 and U343; however, this effect was less prominent in PTEN mutant GB cells (Figure 2A). This data may suggest PTEN is a key mediator in Smurf1 signaling pathway. To test our rationale that blockage of Smurf1 could inhibit cell growth in PTEN wild-type GB cells, we established Smurf1-silenced sublines LN229 and LNZ308 using shSmurf1 (Figure 2B).

Smurf1 knockdown caused a significant decline in LN229 cell proliferation and growth (Figure 2C), but not in LNZ308 cells (Figure 2D), suggesting a tumor-promoting role of Smurf1 in PTEN wild-type GBs. The

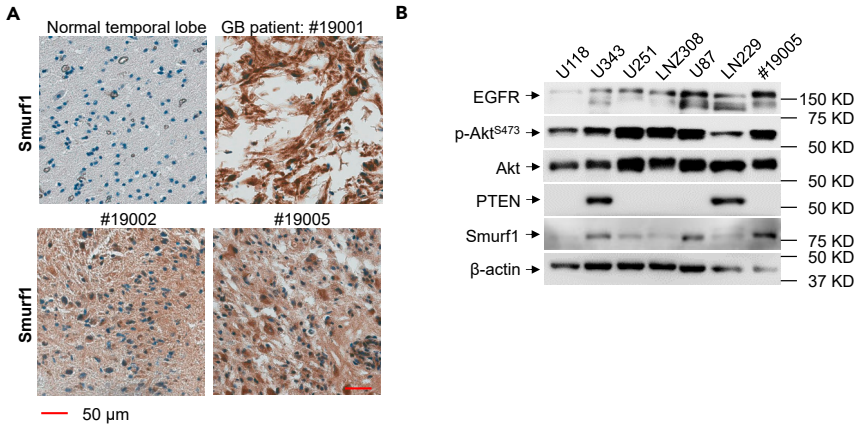

Figure 1. Smurf1 is elevated in GB cells

(A) Immunohistochemistry (IHC) was performed for Smurf1 protein expression in GB patient tissues and in the normal temporal lobe. Tissues were first sectioned, and then sections were probed with primary antibodies against Smurf1. Target protein expression was evaluated via indirect detection using a labeled secondary antibody. After staining with hematoxylin, the antigen-antibody complex was visualized under a bright-field microscope. In IHC stained images brown tint shows positive immunoreactivity for Smurf1 antigen. Scale bars, 50 μm.

(B) Different tumor cells, including PTEN-wt (LN229, U343), and PTEN-mut (U251, LNZ308, U87, U118, and #19005) GB cells were grown under standard culture conditions described in methods. For expression analysis, cells were lysed and whole-cell lysates were examined through Western blotting for the expression of EGFR, p-Akt^{S473}, Akt, PTEN, Smurf1, and β-actin proteins. Results shown here represent three independent experiments.

above data support the hypothesis that Smurf1's oncogenic functions are dependent on PTEN. To further confirm this, we used LN229 and U343 PTEN wild-type GB cells transfected with shSmurf1. We compared the pattern of tyrosine phosphorylation in whole-cell lysates of GB-shSmurf1 and GB-shPLKO cells. Data show Smurf1 knockdown was associated with globally decreased phosphotyrosine (pY) levels in LN229 and U343 (Figure 2E). Most interestingly, p-Akt and p-p70S6K, which are the key regulatory proteins of the PI3K/mTOR signaling pathway, were reduced in LN229-shSmurf1 cells (Figure 2F), indicating that targeting Smurf1 can be a potential strategy to inhibit PI3K/Akt signaling pathway mediated tumor growth.

Smurf1 is an oncogenic driver in the EGFR/PI3K/Akt pathway

To further investigate the phenotypic difference between PTEN wild-type and PTEN mutant cells after Smurf1 knockdown, we measured EGFR signaling protein expression under starvation and growth stimulation conditions. We noticed that Smurf1 knockdown caused a sharp decline in p-Akt expression in PTEN wild-type GB cells (Figures 3A and 3B), supporting the notion about oncogenic implications of Smurf1. In comparison, Smurf1 knockdown in PTEN mutant cells did not affect p-Akt levels in basal or EGF-stimulated conditions (Figures 3C and 3D). This shows Smurf1 plays a supporting role in cellular growth that may be regulated by PTEN via the EGFR pathway. Additional data not shown from PTEN mutant cells (U87, #19005) supports these findings showing that suppression of Smurf1 reduces EGFR signaling in PTEN wild-type cells.

Smurf1 labels PTEN for degradation via ubiquitination

Given the negative impact of Smurf1 knockdown on p-Akt levels in wild-type PTEN cells, we determined if Smurf1 affects the stability of PTEN. Data show p-Akt levels were not affected in LN229-shSmurf1 cells when PTEN was knocked down (Figure 4A). In addition, PTEN protein levels modestly increased after Smurf1 knockdown in LN229-shSmurf1 cells with or without protein synthesis inhibitor cycloheximide (CHX) treatment (Figure 4B).

Considering Smurf1 is an E3 ligase, we assume that Smurf1 may be involved in PTEN degradation. Firstly, we conducted binding assays *in vitro and in vivo*. Pulldown and Immunoprecipitation (IP) results showed that Smurf1 binds to PTEN (Figures 4C and 4D). In addition, the level of PTEN ubiquitination is decreased in shSmurf1 cells under MG132 treatment, and PTEN ubiquitination is increased after Smurf1 overexpression (Figure 4E), advocating the significant role of Smurf1 in PTEN degradation.

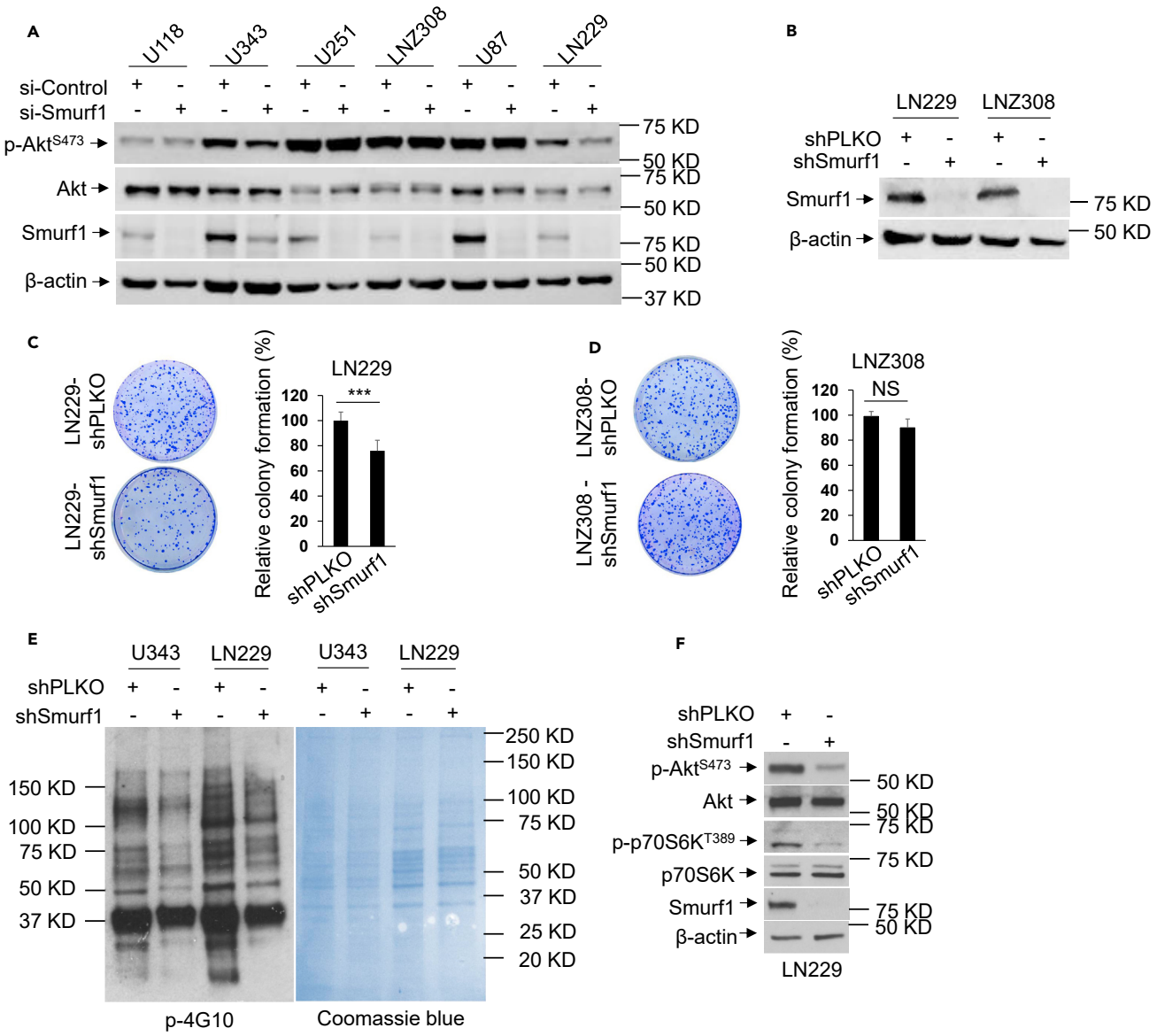

Figure 2. Depletion of Smurf1 decreased GB cell viability

(A) PTEN-wt (LN229 and U343) and PTEN-mut (U118, U251, LNZ308, and U87) GB cell lines were stably transfected with si-Control or si-Smurf1. Western blotting was employed to detect target proteins p-Akt, Akt, Smurf1, and β-actin. Five independent experiments showed similar protein expressions.

(B) The expression of Smurf1 in Smurf1 shRNA-transduced LN229 and LNZ308 cells was examined by Western blotting. Blots show that shSmurf1 effectively knocked down Smurf1.

(C) Anti-proliferative effect of Smurf1 silencing was measured through clonogenic assay. Crystal violet-stained cells represent proliferation and colony formation following shPLKO and shSmurf1 transfection in the LN229 cell line. Smurf1 loss significantly reduces the colony formation capability of LN229 cells (***, $P < 0.001$). Data shown here are means ± SEM of five independent experiments.

(D) Anti-proliferative effect of Smurf1 silencing was measured through clonogenic assay. Crystal violet-stained cells represent proliferation and colony formation following shPLKO and shSmurf1 transfection in the LNZ308 cell line. No significant impact on colony formation potential of LNZ308 cells was observed after Smurf1 knockdown (NS, $P > 0.05$). Data shown here are means ± SEM of five independent experiments.

(E) Comparison of the tyrosine phosphorylation pattern. Western blot of phospho-4G10 in control and Smurf1 shRNA-transduced U343 and LN229 cell lines confirmed that Smurf1 loss causes decreased phosphotyrosine levels.

(F) Analysis of protein expressions in shSmurf1 transfected LN229 cells. Blots show that Smurf1 knockdown in LN229 cells is associated with decline in the expressions of p-Akt and p-p70S6K, which are key regulatory proteins of PI3K/Akt pathway.

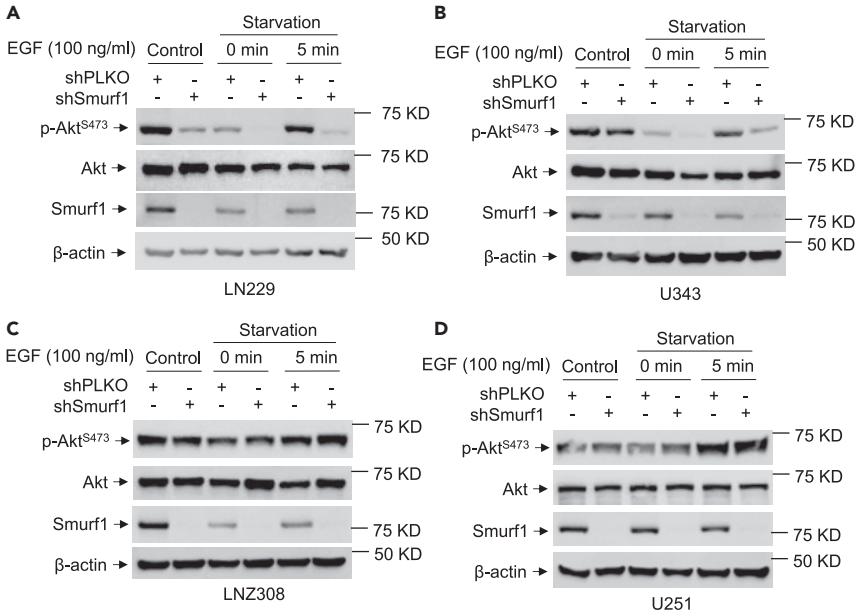

Figure 3. Smurf1 knockdown reduced PTEN dependent EGF signaling

(A–D) GB cell lines: (A) PTEN-wt LN229 cells; (B) PTEN-wt U343 cells; (C) PTEN-mut LNZ308 cells; and (D) PTEN-mut U251 cells were stably transfected with shPLKO or shSmurf1, followed by starvation in serum and growth factor free medium for 48 h and stimulation for 5 min with 100 ng/mL EGF. Immunoblotting is performed on the whole cell lysates to check Smurf1, Akt, and p-Akt levels. In PTEN-wt cells, Smurf1 loss significantly altered the level of p-Akt under analysis; however, PTEN-mut did not show a notable response. All data are presented from three independent experiments, and similar results were obtained.

Suppression of Smurf1 sensitizes GB cells to Torin1 and significantly reduced viability

Smurf1 mediated PTEN loss promotes sustained PI3K/Akt/mTOR signaling that confers resistance to cancer therapeutics. Previous reports suggest PTEN loss promotes resistance to kinase inhibitors of the PI3K signaling pathway (Navarro et al., 2015; She et al., 2005). Consistent with this notion, increased PTEN expression is a strategy to reverse drug resistance. Here, we evaluated whether Smurf1 knockdown can enhance the cytotoxicity of mTORC1/mTORC2 inhibitor Torin1. Data show Torin1 combined with shSmurf1 further decreased p-Akt compared to Torin1 treatment alone (Figure 4F). Of note, Torin1 also downregulated the expression of Smurf1 and p-Akt (Figure 4F). We examined the combined treatment effect on cellular growth of LN229-PLKO and LN229-shSmurf1 through MTT assay. Results show Torin1 moderately suppressed cell growth, which was further reduced when combined with shSmurf1 treatment (Figure 4G).

We proceeded to evaluate if cytotoxicity of Torin1 in PTEN mutant GBs could be recovered by transfection with wild-type PTEN. Results show U251 cells supplemented with PTEN had reduced p-Akt, and after Smurf1 knockdown, p-Akt was further inhibited (Figure 5A). Consistently, U343 had also reduced p-Akt after Smurf1 knockdown (Figure 5B). These results recapitulate data in LN229 normal cells. Importantly, we found the effect of Smurf1 knockdown with Torin1 caused significant cell death in U251 cells supplementary with PTEN (Figure 5C). Again, these findings are in line with data from wild-type PTEN cells. This proves that the Torin1 induced mTOR inhibition is dependent on an intact PTEN/PI3K/Akt pathway.

Importantly, Smurf1 silencing or combination therapies of Smurf1 silencing and Torin1 did not affect the expressions of eukaryotic translation initiation factor 4E (eIF4E)-binding protein 1 (4EBP1) and its phosphorylated form p-4EBP1 compared to corresponding control (Figure 5D). However, a substantial decline in the phosphorylation of another mTORC1 downstream substrate S6 kinase K1 (S6K1, p70S6K) was observed in LN229-shSmurf1 (Figures 2F and 4F). The inhibitory effect of Torin1 on mTOR signaling was potentiated after Smurf1 silencing (Figure 4F). Hence, Torin1 decreases the PI3K/mTOR signaling by blocking the phosphorylation of Akt and S6K1, whereas Smurf1 knockdown blocks S6K1 and elevates the levels of PTEN, which further reduces Akt activation. These results provide a mechanistic explanation for the

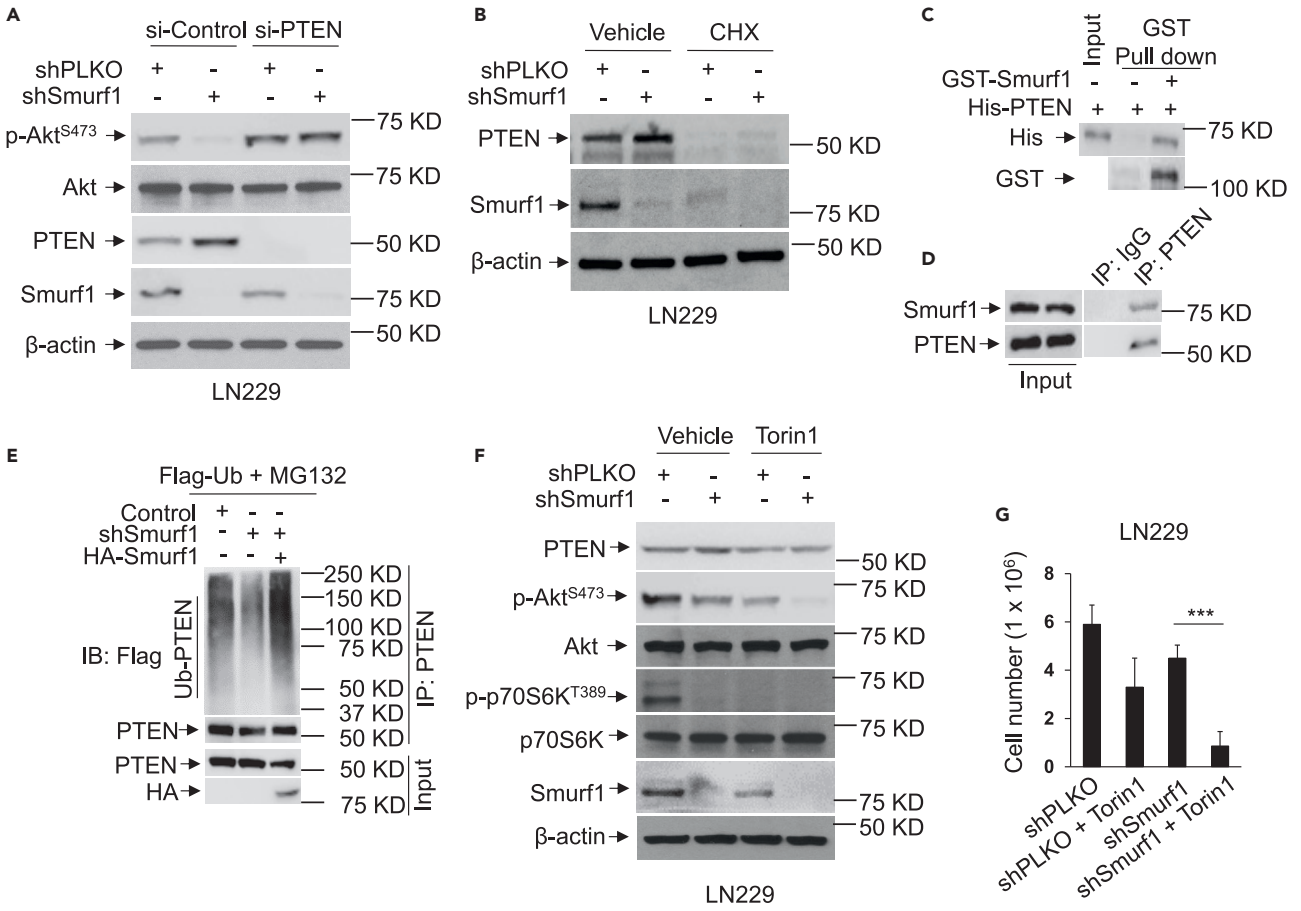

Figure 4. Smurf1 labels PTEN for degradation via ubiquitination and suppression of Smurf1 sensitizes GB cells to Torin1

(A) To validate our hypothesis that Smurf1 exerts its oncogenic effects through PTEN regulation, we transfected LN229 (shSmurf1 and shPLKO) cells with si-Control or si-PTEN for 72 h. Immunoblotting was employed to analyze the PTEN silencing efficacy and expressions of target proteins p-Akt and Akt in cell lysates. Blot shows that Smurf1 knockdown had no effect on p-Akt and Akt protein in si-PTEN treated LN229 (shSmurf1 and shPLKO) cells, verifying that Smurf1 effects on tumors are dependent on PTEN.

(B) Impact of Smurf1 knockdown on PTEN expression was further verified by treating LN229 (shSmurf1 and shPLKO) cells with protein synthesis inhibitor CHX (100 μg/mL) for 24 h. Western blotting recapitulated similar results, showing that expression of PTEN is increased after Smurf1 loss, even in the presence of CHX.

(C) Pull down assay established a direct physical contact between Smurf1 and PTEN.

(D) Immunoprecipitation analysis in LN229 cells using mouse antibody IgG and anti-PTEN antibody also confirmed this interaction.

(E) To assess the involvement of Smurf1 in PTEN ubiquitylation, LN229 cells were treated with shSmurf1 (knockdown) and HA-Smurf1 (silent mutant against shSmurf1) (overexpression) in the presence of proteasome inhibitor MG132. LN229 controls received Flag-ubiquitin. It is evident from the blot that Smurf1 silencing decreases PTEN ubiquitination, whereas HA-Smurf1 induced overexpression of Smurf1 significantly enhanced PTEN ubiquitination even in the presence of shSmurf1 and MG132.

(F) LN229 cells were transfected with shSmurf1 or shPLKO in the presence or absence of mTOR inhibitor Torin1 (500 nM). Western blotting was carried out to study changes in the expression of target proteins, including p-Akt, Akt, p-p70S6K, and p70S6K.

(G) Before cell lysis for expression analysis, MTT assay was performed to evaluate the cytotoxicity of treatments on LN229 GB cells. Similar results were obtained from three independent experiments. All data are presented as means ± SEM (n = 3 in each group). (***, $p < 0.001$).

synergistic inhibitory effects of Smurf1 silencing and Torin1 cotreatment and explain the possible link between Smurf1 loss and rise in the sensitivity of Torin1. Thus, Smurf1 knockdown increases cellular levels of PTEN and alters the sensitivity of mTOR inhibitor Torin1. These results highlight Smurf1 as a druggable vulnerability in PTEN wild-type tumors.

To verify the hypothesis that Smurf1 suppression together with Torin1 has enhanced efficacy compared to the combined use of Smurf1 suppression with rapamycin, we first tested the downstream target

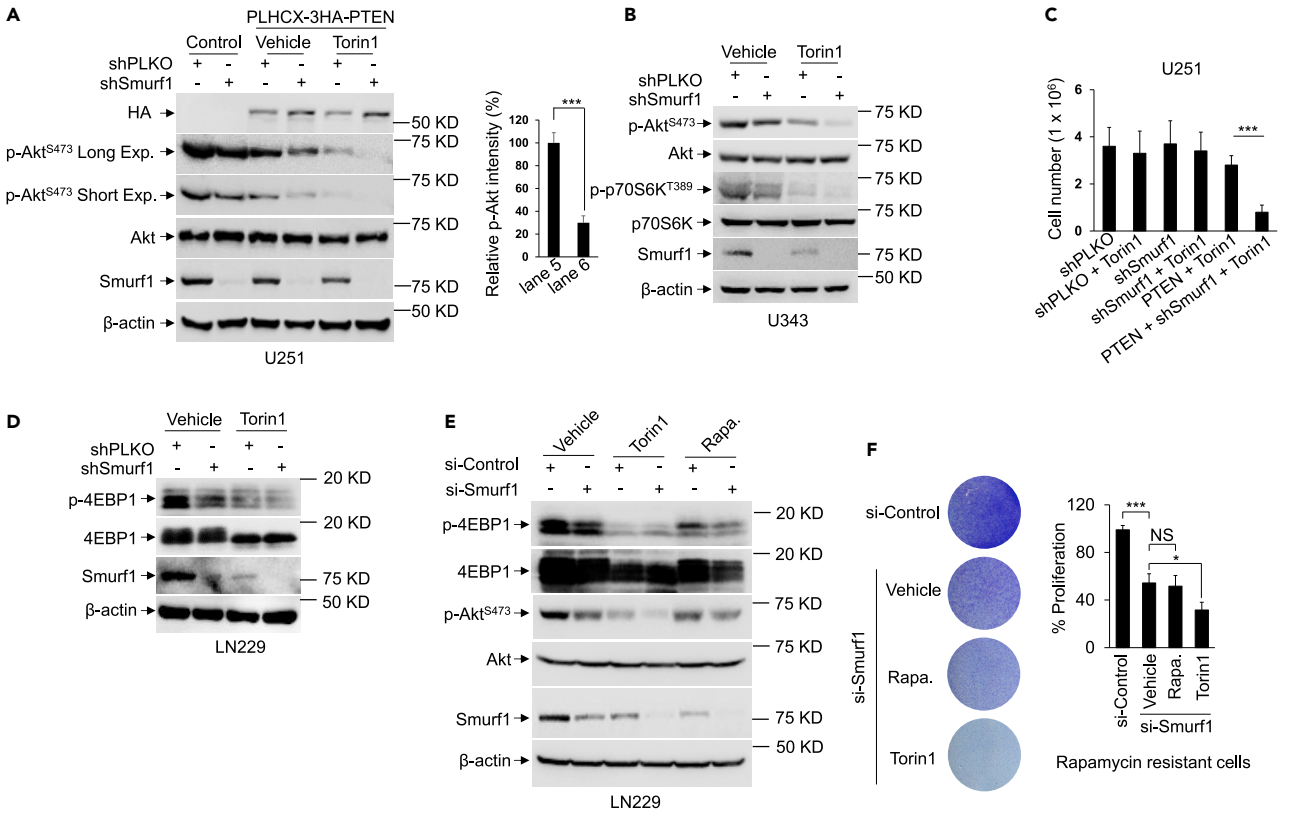

Figure 5. Transfection of wild-type PTEN into mutant GB cells resolved Torin1 cytotoxicity

(A) U251-shSmurf1 and U251-shPLKO cells were transfected with PLHCX-3HA-PTEN followed by treatment with/without Torin1 (500 nM). To measure protein expressions, Western blotting was done for p-Akt, Akt, Smurf1, and β-actin. The graph on the right showed the relative p-Akt intensity of lane 5 and lane 6.

(B) U343-shSmurf1 and U343-shPLKO cells treated with/without Torin1 (500 nM). To measure protein expressions, Western blotting was done for p-Akt, Akt, p-p70S6K, p70S6K, Smurf1, and β-actin.

(C) The number of cells in each group was counted through colorimetric MTT assay before cell collection or lysis.

(D) Levels of the 4EBP1 and p-4EBP1 in LN229-shPLKO and LN229-shSmurf1 cells, in the presence or absence of Torin1 treatment, were determined by Western blotting. β-actin was taken as a loading control.

(E) LN229 with or without Smurf1 knockdown treated with/without Torin1 (500 nM) or Rapa.

(100 nM). To measure protein expressions, Western blotting was done for p-4EBP1, 4EBP1, p-Akt, Akt, Smurf1, and β-actin.

(F) Anti-proliferative effect was measured through clonogenic assay. Crystal violet-stained cells represent proliferation and colony formation following shPLKO and shSmurf1 transfection in Rapamycin resistant cells with or without Torin1 (500 nM) or Rapamycin (100 nM) treatment. Rapamycin resistant cell lines were built by treating LN229 cells in a medium gradually supplemented with Rapamycin for 2 weeks; results shown here represent similar data from three independent experiments; mean ± SEM (n = 3). (NS, $p > 0.05$; *, $p < 0.05$; ***, $p < 0.001$)

phosphorylation level. Consistently, both phosphorylation of Akt and 4EBP1 were strongly suppressed in the treatment of si-Smurf1 with Torin1 compared to with Rapamycin (Figure 5E). Importantly, the combination treatment of si-Smurf1 with Torin1 further decreased cell colony formation and apoptotic cells in Rapamycin resistant cell line, suggesting that consistent blocking of 4EBP1 phosphorylation and mTORC2 kinase may result in synergically enhancing the cytotoxicity on GB cells under the Smurf1 suppression (Figure 5F).

Smurf1 knockdown inhibits the cell cycle and promotes apoptosis

To analyze whether Smurf1 knockdown affects the cell cycle, we immuno-stained LN229-shPLKO and LN229-shSmurf1 cells with Ki67 to visualize proliferating cells. Results showed a notable reduction in the proliferation rate of cancer cells, as evidenced by a sharp decline in the Ki67 positive cells (Figure 6A). Most importantly, flow cytometry data show cotreatment of Smurf1 suppression and Torin1 resulted in significantly more G0/G1 phase arrest and apoptotic cells than monotherapy (Figures 6B and 6C).

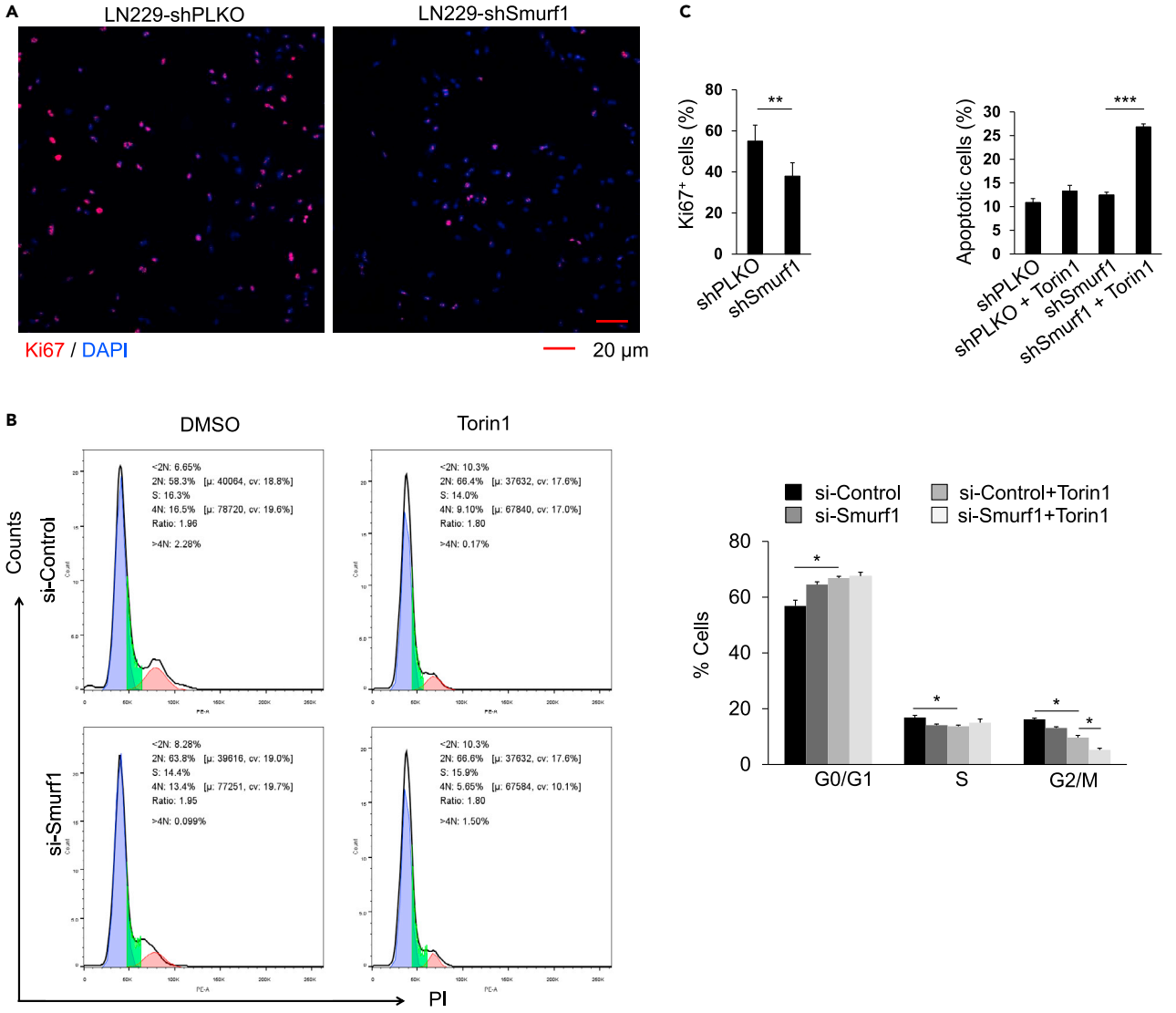

Figure 6. Smurf1 knockdown combined with Torin1 treatment inhibited the cell cycle and promoted apoptosis

(A) Representative immunofluorescence staining of Ki67 (red) in PTEN-wt GB cells, LN229 (shSmurf1 and shPLKO). The nuclear localization was verified by staining (DAPI; blue). The number of Ki67^{+} cells was counted in each section. **, $P < 0.01$.

(B) Cell cycle analysis through flow cytometry. The impact of si-Smurf1 and Torin1 treatments on cell cycle progression was measured in PTEN-wt LN229 GB cells. Cell quantification data in each phase of the cell cycle was represented on the right.

(C) Apoptotic efficiency of treatments was analyzed in PTEN-wt GB cells LN229 (shSmurf1 and shPLKO) with or without Torin1 treatment. Cells were stained using Annexin V-FITC/PI kit followed by apoptosis analysis through flow cytometry. All data are displayed as means ± SEM (n = 5).

Loss of Smurf1 paced elimination of tumors in an orthotopic mouse model

To analyze the *in vivo* response to Smurf1 knockdown and mTOR inhibitor Torin1, we injected firefly luciferase tagged LN229-shSmurf1 and LN229-shPLKO cells directly into the cerebrum of mice brain. Consistent with the results of previous experiments, LN229-shSmurf1 displayed significant tumor growth delay in animals and increased response to Torin1 treatment (Figures 7A and 7B). To confirm the molecular mechanism underlying observed changes in tumor growth, tumor tissue sections from end-stage mice were immunostained for PTEN protein. Relative to tumors from untreated mice, tumors from the Smurf1-knockdown cohort displayed upregulation of PTEN signaling and hence reduced mTOR signaling (Figure 7C, third panel). Tumors from Torin1-treated mice did not cause a significant elevation in PTEN levels and tumor reduction (Figure 7C, second panel). Notably, tumors from shSmurf1+Torin1-treated mice exhibit the

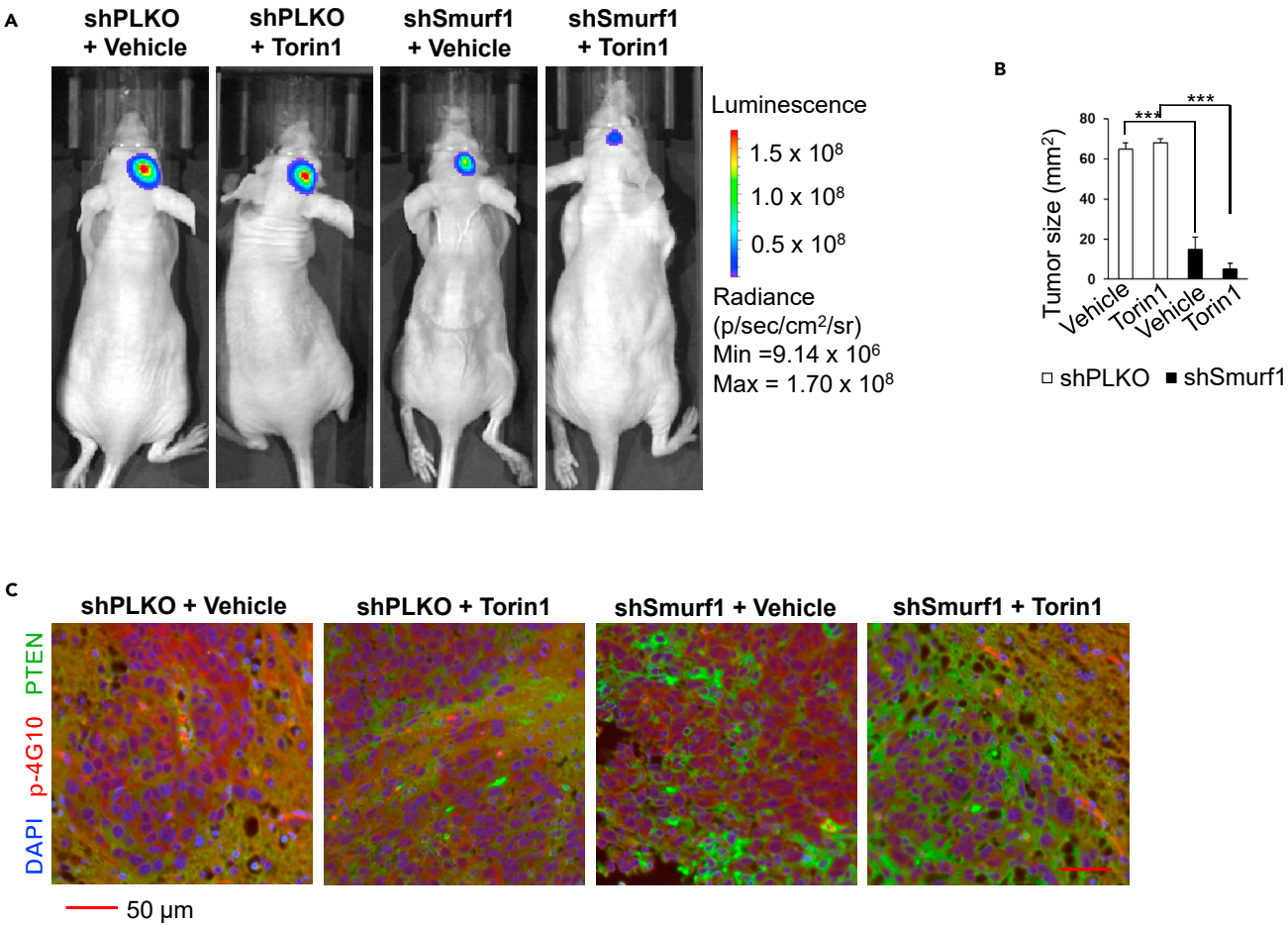

Figure 7. Cotreatment with Smurf1 silencing and Torin1 produced a synergistic inhibitory effect in an orthotopic mouse model

(A–C) LN229 (shSmurf1 or shPLKO) tumor cells were intracranially implanted into the female BALB/c nude mice (n = 15; 5 × 10^5 tumor cells per animal), which were then randomized into two groups. Starting from ten days post-implantation, mice in each group received 5 times/week intraperitoneal injection of vehicle (75% ethanol +25% PBS) or Torin1 (20 mg/kg). IVIS imaging performed after three weeks of treatment shows *in vivo* tumor growth (n = 15/group) (A); tumor size in mm^2 (n = 5/group in replicates) (B); and immunofluorescence staining of DAPI, p-4G10 and PTEN (n = 3/group in replicates) (C).

most pronounced changes in PTEN expression and mTOR signaling (Figure 7C, fourth panel). We conclude that Smurf1 knockdown not only reverses PI3K/Akt signaling in PTEN wild-type cells but also sensitizes GB cells to Torin1 induced inhibition of mTOR signaling.

DISCUSSION

Drug resistance in GB is a common phenomenon. To date, inhibitors targeting different PI3K/Akt/mTOR pathway components have not significantly improved GB prognosis (Cancer Genome Atlas Research, 2008; Stupp et al., 2005; Zhao et al., 2017). Genetic or posttranslational loss of PTEN is correlated with higher drug resistance. For example, Torin1 treatment led to compensatory activation of PI3K/Akt/mTOR pathway in PTEN-deficient patients during Phase I clinical trial (Cloughesy et al., 2008). EGFR kinase inhibitor is an ineffective strategy in PTEN-deficient tumors (Mellinghoff et al., 2005; VanderLaan et al., 2017). Hence, increased PTEN expression is a characteristic of the reversal of drug resistance to tyrosine kinase inhibitors in GB patients with reduced PTEN. Pharmacological inactivation of NEDD4 family E3 ligase WWP1 activates PTEN and suppresses PI3K/Akt/mTOR pathway-driven tumor progression (Lee et al., 2019). To date, the effect of E3 ligase Smurf1 suppression on the chemotherapeutic efficacy of Torin1 has not been studied in human GB. Given that the PI3K/Akt network is commonly implicated in oncogenic mTORC1 signaling in the mTOR-insensitive cancers (Shaw and Cantley, 2006), we proposed that resistance to mTOR inhibitors can be reversed by Smurf1 silencing in cancer cells. So how could Smurf1 silencing sensitize cancer cells to a mTORC1/C2 inhibitor Torin1?

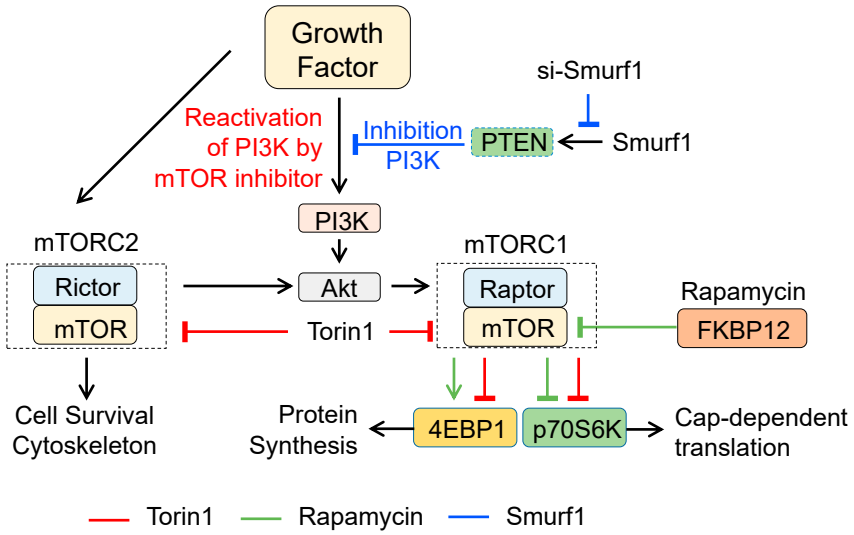

Figure 8. Targeting Smurf1 promotes Torin1 efficacy in PTEN-wild type GB

Allosteric inhibitors of mTORC1 rapamycin are largely ineffective in inhibiting mTORC2 activity. In addition, 4EBP1 is rephosphorylated to long-term rapamycin treatment. Torin1 potently inhibits mTORC1 and mTORC2. We tested the enhanced efficacy of Torin1 by suppression of Smurf1 through sustained inhibition of 4EBP1 phosphorylation.

Smurf1 expression negatively regulates PTEN, a potent antagonizer of PI3K/Akt activity. We found that Smurf1 knockdown rescues PTEN from ubiquitylation mediated degradation and reduced p-Akt levels. To further validate if Smurf1 is implicated in aberrant EGFR signaling, we tested EGF-stimulated signaling pathways in different GB cells after starvation with or without Smurf1 silencing. The suppression of Smurf1 inhibits EGFR signaling in PTEN wild-type GB cells, suggesting Smurf1 oncogenic effects are PTEN dependent. Mechanistically, Smurf1 directly ubiquitylates and degrades PTEN *in vitro*. Our data show Smurf1 knockdown along with Torin1 treatment significantly increased drug sensitivity in GB cells compared to Torin1 alone. In addition, a synthetically lethal effect was also verified in the orthotopic GB mouse model. To summarize, Smurf1 silencing antagonized PI3K/Akt/mTOR signaling, culminating in cell cycle inhibition and reduced colony formation. This suggests Smurf1 suppression holds the potential of sensitizing glioma cells to Torin1. For a more logical explanation of how Smurf1 silencing can alleviate resistance to mTOR inhibitors, causes of resistance should be explored.

Resistance to mTOR inhibitors may emerge from various mechanisms: loss of negative feedback-loops (S6K1/IRS-1 and S6K1/mTORC2) (Ghosh and Kapur, 2017); mutations in the kinase domains of mTOR (gain of function mutation M2327I); compensatory activation, or overactivation of some signaling cascades (PI3K/Akt, MEK/ERK); and increased eIF4E/4E-BPs ratio (Formisano et al., 2020). Of the two mTOR complexes, mTORC1 usually regulates cellular functions through its downstream substrates S6K1 and 4EBP1 (Ito et al., 2016). S6K1 and 4EBP1 mainly trigger protein synthesis and cell proliferation, respectively. mTORC2 also influences the pathway indirectly by phosphorylating and activating Akt (Dowling et al., 2010). Although phosphorylation of 4EBP1 seems to be mainly controlled by the mTORC1 pathway, other unknown kinases (CDK1) or mechanisms (ATM/p53) also regulate its activity (She et al., 2010). This is because various phosphorylation sites in 4EBP1 may be partly insensitive or respond differently to Torin1 and rapamycin. Rapamycin is generally accepted to block mTORC1 mediated 4EBP1 phosphorylation and mRNA translational, as well as phosphorylation of S6K1. For instance, we reported rapamycin-induced potent inhibition of S6K1 phosphorylation in GB cells (Xia et al., 2020). Some studies demonstrated transient inhibition or even stimulation of mTORC1/4EBP1 axis after rapamycin treatment (Choo et al., 2008; Ogasawara and Suginohara, 2018; Shaw and Cantley, 2006). Furthermore, rapamycin-induced inhibition of S6K1 abrogates negative feedback loops (S6K1/Rictor, S6K1/IRS1, etc.), leading to hyperactivation of the PI3K/Akt pathway. Hence, mTOR catalytic inhibitor Torin1 could be more effective in rapamycin-resistant phenotype (Figure 8).

This study demonstrates that Torin1, alone or in combination with shSmurf1, affects 4EBP1 phosphorylation. Together, Torin1 treatment significantly inhibited S6K1 phosphorylation that was further potentiated in the presence of Smurf1 silencing. Importantly, inhibition of S6K1 and 4EBP1 did not disrupt the negative

feedback loops as indicated by consistent low levels of p-Akt. It shows that Smurf1 suppression effects are not mediated by mTORC1/4EBP1 instead of the Akt/mTORC1/S6K1 axis (Figure 5D). Both Smurf1 loss and Torin1 treatment target S6K1 and Akt signaling as measured by their phosphorylation. These findings provide a possible mechanistic explanation for the synergistic inhibitory effects of Smurf1 silencing and Torin1 treatment (Figure 8). Further studies are warranted to quantify the drug synergy by using the Chou-Talalay method (Chou, 2010; Peterson and Novick, 2007). Of note, 1) degradation of PTEN also contribute its role in nucleus independent of its cytoplasmic activities (Lee et al., 2018; Xie et al., 2021); and 2) that levels of HIF-1 a protein were maintained in hypoxic cells exposed toward rapamycin emphasis the important role of tumor microenvironmental glioma cells under selective pressure to maintain HIF-1 a-dependent neoangiogenesis (Ronellenfitsch et al., 2009). Further studies are warranted to reveal in-depth mechanisms (including PTEN nucleus and cytoplasmic role) underlying self-autonomous effect of Smurf1 knockdown mediated sensitization of Torin1 by using multiple patient-derived glioblastoma cell cultures and patient derived xenografts.

Conclusions

In conclusion, this study reveals Smurf1 as a novel druggable vulnerability and encourages the combination of mTOR inhibitors with Smurf1 suppression for cancer patients experiencing primary drug resistance. Amplification of Smurf1 renders tumor cells resistant to various small molecule inhibitors of the EGFR pathway and promotes tumor progression by sustaining the Akt/mTOR signaling in the presence of PTEN. Intriguingly, our data imply that overexpression of Smurf1 results in high levels of p-Akt, leading to a higher proliferation rate and reduced sensitivity to mTOR inhibition. Mechanistically, Smurf1 mediates ubiquitylation and proteasomal degradation of PTEN. Loss of PTEN enhances the growth of tumors in GB cells and mouse models and confers resistance to small molecule inhibitors via overactivation of the PI3K/Akt/mTOR signaling. Treatment with Smurf1 suppression leads to reduced GB growth and increased cell-cycle arrest and apoptosis. These findings suggest Smurf1 silencing combined with Torin1 treatment could be a promising approach for the treatment of PTEN wild-type GB.

ABBREVIATIONS

Smurf1	SMAD Specific E3 Ubiquitin Protein Ligase 1
GB	Glioblastoma
EGFR	Epidermal growth factor receptor
PTEN	Phosphatase and tensin homolog
PI3K	Phosphatidylinositol 3-kinase (PKB)
Akt	Serine/threonine kinase-specific protein kinase, also called protein kinase B
mTOR	Mammalian target of rapamycin
mTORC1	Mammalian target of rapamycin complex 1
mTORC2	Mammalian target of rapamycin complex 2
S6K1	S6 kinase K1
4EBP1	Eukaryotic translation initiation factor 4E-binding protein 1
RTK	Receptor tyrosine kinase
PIP2	Phosphatidylinositol 4,5-bisphosphate
PIP3	Phosphatidylinositol (3,4,5)-trisphosphate
MEK	Mitogen-activated protein kinase/ERK kinase
ERK	Extracellular-signal-regulated kinase
IRS1	Insulin Receptor Substrate 1
Rictor	Rapamycin-insensitive companion of mammalian target of rapamycin

STAR★METHODS

Detailed methods are provided in the online version of this paper and include the following:

- KEY RESOURCES TABLE
- RESOURCE AVAILABILITY
  - Lead contact

ACKNOWLEDGMENTS

We thank the Analysis & Testing Center, Beijing Institute of Technology; and the biological and medical engineering core facilities of the School of Life Science, Beijing Institute of Technology. This work was supported by grants from the Natural Science Foundation of Beijing Municipality (Z190018), The National Natural Science Foundation of China (81870123), Beijing Institute of Technology Research Fund Program for Young Scholars (XSQD-202110002), and the National Science Foundation for Young Scientists of China (81902545).

AUTHOR CONTRIBUTIONS

Conceptualization, Lei Dong; Data curation, Qin Xia; Formal analysis, Qin Xia; Funding acquisition, Qin Xia, and Lei Dong; Investigation, Wenxuan Li, Sakhawat Ali, Mengchuan Xu, and Yang Li; Methodology, Qin Xia, and Lei Dong; Project administration, Qin Xia, and Lei Dong; Resources, Qin Xia, and Lei Dong; Software, Qin Xia, Wenxuan Li, Sakhawat Ali, Mengchuan Xu, and Yang Li; Supervision, Lei Dong; Validation, Qin Xia; Visualization, Qin Xia, Wenxuan Li, Mengchuan Xu, and Yang Li; Writing – original draft, Qin Xia, and Lei Dong; Writing - review & editing, Qin Xia,Lei Dong, Shengzhen Li, Xinyi Meng, Liqun Liu.

DECLARATION OF INTERESTS

The authors declare no competing interests.

Received: June 1, 2021
Revised: September 13, 2021
Accepted: November 23, 2021
Published: December 17, 2021

REFERENCES

Brennan, C.W., Verhaak, R.G., McKenna, A., Campos, B., Noushmehr, H., Salama, S.R., Zheng, S., Chakravarty, D., Sanborn, J.Z., Berman, S.H., et al. (2013). The somatic genomic landscape of glioblastoma. Cell *155*, 462–477.

Cancer Genome Atlas Research, N. (2008). Comprehensive genomic characterization defines human glioblastoma genes and core pathways. Nature *455*, 1061–1068.

Chang, H., Zhang, J., Miao, Z., Ding, Y., Xu, X., Zhao, X., Xu, P., Wang, Q., and Lin, Y. (2018). Suppression of the Smurf1 expression inhibits tumor progression in gliomas. Cell. Mol. Neurobiol. *38*, 421–430.

Chen, P., Zhao, D., Li, J., Liang, X., Li, J., Chang, A., Henry, V.K., Lan, Z., Spring, D.J., Rao, G., et al. (2019). Symbiotic macrophage-glioma cell interactions reveal synthetic lethality in PTEN-null glioma. Cancer Cell *35*, 868–884 e866.

Choo, A.Y., Yoon, S.-O., Kim, S.G., Roux, P.P., and Blenis, J. (2008). Rapamycin differentially inhibits S6Ks and 4E-BP1 to mediate cell-type-specific repression of mRNA translation. Proc. Natl. Acad. Sci. *105*, 17414–17419.

Chou, T.C. (2010). Drug combination studies and their synergy quantification using the Chou-Talalay method. Cancer Res. *70*, 440–446.

Cloughesy, T.F., Yoshimoto, K., Nghiemphu, P., Brown, K., Dang, J., Zhu, S., Hsueh, T., Chen, Y., Wang, W., Youngkin, D., et al. (2008). Antitumor activity of rapamycin in a Phase I trial for patients with recurrent PTEN-deficient glioblastoma. PLoS Med. *5*, e8.

Dowling, R.J., Topisirovic, I., Alain, T., Bidinosti, M., Fonseca, B.D., Petroulakis, E., Wang, X., Larsson, O., Selvaraj, A., and Liu, Y. (2010). mTORC1-mediated cell proliferation, but not cell growth, controlled by the 4E-BPs. Science *328*, 1172–1176.

Formisano, L., Napolitano, F., Rosa, R., D'Amato, V., Servetto, A., Marciano, R., De Placido, P., Bianco, C., and Bianco, R. (2020). Mechanisms of

resistance to mTOR inhibitors. Crit. Rev. Oncol. Hematol. *147*, 102886.

Furnari, F.B., Lin, H., Huang, H.S., and Cavenee, W.K. (1997). Growth suppression of glioma cells by PTEN requires a functional phosphatase catalytic domain. Proc. Natl. Acad. Sci. U S A *94*, 12479–12484.

Furnari, F.B., Fenton, T., Bachoo, R.M., Mukasa, A., Stommel, J.M., Stegh, A., Hahn, W.C., Ligon, K.L., Louis, D.N., Brennan, C., et al. (2007). Malignant astrocytic glioma: genetics, biology, and paths to treatment. Genes Dev. *21*, 2683–2710.

Ghosh, J., and Kapur, R. (2017). Role of mTORC1-S6K1 signaling pathway in regulation of hematopoietic stem cell and acute myeloid leukemia. Exp. Hematol. *50*, 13–21.

Ishii, N., Maier, D., Merlo, A., Tada, M., Sawamura, Y., Diserens, A.C., and Van Meir, E.G. (1999). Frequent co-alterations of TP53, p16/CDKN2A, p14ARF, PTEN tumor suppressor genes in human glioma cell lines. Brain Pathol. *9*, 469–479.

Ito, H., Ichiyanagi, O., Naito, S., Bilim, V.N., Tomita, Y., Kato, T., Nagaoka, A., and Tsuchiya, N. (2016). GSK-3 directly regulates phospho-4EBP1 in renal cell carcinoma cell-line: an intrinsic subcellular mechanism for resistance to mTORC1 inhibition. BMC Cancer *16*, 1–12.

Lee, Y.R., Chen, M., and Pandolfi, P.P. (2018). The functions and regulation of the PTEN tumour suppressor: new modes and prospects. Nat. Rev. Mol. Cell Biol. *19*, 547–562.

Lee, Y.R., Chen, M., Lee, J.D., Zhang, J., Lin, S.Y., Fu, T.M., Chen, H., Ishikawa, T., Chiang, S.Y., Katon, J., et al. (2019). Reactivation of PTEN tumor suppressor for cancer treatment through inhibition of a MYC-WWP1 inhibitory pathway. Science *364*, eaau0159.

Li, J., Yen, C., Liaw, D., Podsypanina, K., Bose, S., Wang, S.I., Puc, J., Miliaresis, C., Rodgers, L., McCombie, R., et al. (1997). PTEN, a putative protein tyrosine phosphatase gene mutated in human brain, breast, and prostate cancer. Science *275*, 1943–1947.

Melick, C.H., and Jewell, J.L. (2020). Small molecule H89 renders the phosphorylation of S6K1 and AKT resistant to mTOR inhibitors. Biochem. J. *477*, 1847–1863.

Mellinghoff, I.K., Wang, M.Y., Vivanco, I., Haas-Kogan, D.A., Zhu, S., Dia, E.Q., Lu, K.V., Yoshimoto, K., Huang, J.H., Chute, D.J., et al. (2005). Molecular determinants of the response of glioblastomas to EGFR kinase inhibitors. N. Engl. J. Med. *353*, 2012–2024.

Meyer, M.A. (2008). Malignant gliomas in adults. N. Engl. J. Med. *359*, 1850.

Moores, S.L., Chiu, M.L., Bushey, B.S., Chevalier, K., Luistro, L., Dorn, K., Brezski, R.J., Haytko, P., Kelly, T., Wu, S.J., et al. (2016). A novel bispecific antibody targeting EGFR and cMet is effective against EGFR inhibitor-resistant lung tumors. Cancer Res. *76*, 3942–3953.

Navarro, L., Gil-Benso, R., Megias, J., Munoz-Hidalgo, L., San-Miguel, T., Callaghan, R.C., Gonzalez-Darder, J.M., Lopez-Gines, C., and Cerda-Nicolas, M.J. (2015). Alteration of major vault protein in human glioblastoma and its relation with EGFR and PTEN status. Neuroscience *297*, 243–251.

Ogasawara, R., and Suginohara, T. (2018). Rapamycin-insensitive mechanistic target of rapamycin regulates basal and resistance exercise-induced muscle protein synthesis. FASEB J. *32*, 5824–5834.

Paez, J.G., Janne, P.A., Lee, J.C., Tracy, S., Greulich, H., Gabriel, S., Herman, P., Kaye, F.J., Lindeman, N., Boggon, T.J., et al. (2004). EGFR mutations in lung cancer: correlation with clinical response to gefitinib therapy. Science *304*, 1497–1500.

Peterson, J.J., and Novick, S.J. (2007). Nonlinear blending: a useful general concept for the assessment of combination drug synergy. J. Recept. Signal Transduct. Res. *27*, 125–146.

Ronellenfitsch, M.W., Brucker, D.P., Burger, M.C., Wolking, S., Tritschler, F., Rieger, J., Wick, W., Weller, M., and Steinbach, J.P. (2009). Antagonism of the mammalian target of rapamycin selectively mediates metabolic effects of epidermal growth factor receptor inhibition and protects human malignant glioma cells from hypoxia-induced cell death. Brain *132*, 1509–1522.

Shaw, R.J., and Cantley, L.C. (2006). Ras, PI (3) K and mTOR signalling controls tumour cell growth. Nature *441*, 424–430.

She, Q.B., Solit, D.B., Ye, Q., O'Reilly, K.E., Lobo, J., and Rosen, N. (2005). The BAD protein integrates survival signaling by EGFR/MAPK and PI3K/Akt kinase pathways in PTEN-deficient tumor cells. Cancer Cell *8*, 287–297.

She, Q.-B., Halilovic, E., Ye, Q., Zhen, W., Shirasawa, S., Sasazuki, T., Solit, D.B., and Rosen, N. (2010). 4E-BP1 is a key effector of the oncogenic activation of the AKT and ERK signaling pathways that integrates their function in tumors. Cancer Cell *18*, 39–51.

Stupp, R., Mason, W.P., van den Bent, M.J., Weller, M., Fisher, B., Taphoorn, M.J., Belanger, K., Brandes, A.A., Marosi, C., Bogdahn, U., et al. (2005). Radiotherapy plus concomitant and adjuvant temozolomide for glioblastoma. N. Engl. J. Med. *352*, 987–996.

Thoreen, C.C., Kang, S.A., Chang, J.W., Liu, Q., Zhang, J., Gao, Y., Reichling, L.J., Sim, T., Sabatini, D.M., and Gray, N.S. (2009). An ATP-competitive mammalian target of rapamycin inhibitor reveals rapamycin-resistant functions of mTORC1. J. Biol. Chem. *284*, 8023–8032.

VanderLaan, P.A., Rangachari, D., Mockus, S.M., Spotlow, V., Reddi, H.V., Malcolm, J., Huberman, M.S., Joseph, L.J., Kobayashi, S.S., and Costa, D.B. (2017). Mutations in TP53, PIK3CA, PTEN and other genes in EGFR mutated lung cancers: correlation with clinical outcomes. Lung Cancer *106*, 17–21.

Xia, Q., Zhang, H., Zhang, P., Li, Y., Xu, M., Li, X., Li, X., and Dong, L. (2020). Oncogenic Smurf1 promotes PTEN wild-type glioblastoma growth by mediating PTEN ubiquitylation. Oncogene *39*, 5902–5915.

Xie, P., Zhang, M., He, S., Lu, K., Chen, Y., Xing, G., Lu, Y., Liu, P., Li, Y., Wang, S., et al. (2014). The covalent modifier Nedd8 is critical for the activation of Smurf1 ubiquitin ligase in tumorigenesis. Nat. Commun. *5*, 3733.

Xie, P., Peng, Z., Chen, Y., Li, H., Du, M., Tan, Y., Zhang, X., Lu, Z., Cui, C.P., Liu, C.H., et al. (2021). Neddylation of PTEN regulates its nuclear import and promotes tumor development. Cell Res. *31*, 291–311.

Yaish, P., Gazit, A., Gilon, C., and Levitzki, A. (1988). Blocking of EGF-dependent cell proliferation by EGF receptor kinase inhibitors. Science *242*, 933–935.

Yang, Y., Shao, N., Luo, G., Li, L., Zheng, L., Nilsson-Ehle, P., and Xu, N. (2010). Mutations of PTEN gene in gliomas correlate to tumor differentiation and short-term survival rate. Anticancer Res. *30*, 981–985.

Yang, J.M., Schiapparelli, P., Nguyen, H.N., Igarashi, A., Zhang, Q., Abbadi, S., Amzel, L.M., Sesaki, H., Quinones-Hinojosa, A., and Iijima, M. (2017). Characterization of PTEN mutations in brain cancer reveals that pten mono-ubiquitination promotes protein stability and nuclear localization. Oncogene *36*, 3673–3685.

Zhao, H.F., Wang, J., Shao, W., Wu, C.P., Chen, Z.P., To, S.T., and Li, W.P. (2017). Recent advances in the use of PI3K inhibitors for glioblastoma multiforme: current preclinical and clinical development. Mol. Cancer *16*, 100.

STAR★METHODS

KEY RESOURCES TABLE

REAGENT or RESOURCE	SOURCE	IDENTIFIER
Antibodies		
Mouse monoclonal anti-Smurf1	Abcam	Cat#ab57573
Rabbit polyclonal anti-Akt	CST	Cat#9272
Rabbit monoclonal anti-Phospho-Akt (Ser473)	CST	Cat#4060
Mouse monoclonal anti-β-actin	Sigma	Cat#A1978-200
Mouse monoclonal anti-PTEN	Santa	Cat#sc-7974
Rabbit polyclonal anti-PTEN	Proteintech	Cat#10047-1-AP
Mouse monoclonal anti-PTEN	Cascade BioScience	Cat#ABM-2052
Rabbit polyclonal anti-EGFR	CST	Cat#4267
Mouse monoclonal anti-Phosphotyrosine (p-4G10)	EMD Millipore	Cat#5-321X
Mouse monoclonal anti-HA	MBL International	Cat#M180-3
Rabbit polyclonal anti-Ki67	Abcam	Cat#ab15580
Rabbit polyclonal anti-Phospho-p70S6K (Thr389)	CST	Cat#9205
Mouse monoclonal anti-p70S6K	Santa	Cat#sc-8418
Rabbit monoclonal anti-4EBP1	CST	Cat#9644
Rabbit monoclonal anti-Phospho-4EBP1 (Thr37/46)	CST	Cat#2855
Goat anti-Rabbit IgG (H+L) (HRP) Polyclonal	Thermo Fisher	Cat#PI-31460
Goat anti-Mouse IgG (H+L) (HRP) Polyclonal	Thermo Fisher	Cat#PI-31430
Chemicals, peptides, and recombinant proteins		
lipofectamine 2000	Invitrogen	Cat#11668
Polybrene	Solarbio	Cat#H8761
Lipofectamine RNAiMAX reagent	Invitrogen	Cat#13778-075
D-luciferin	Promega	Cat#1041
Experimental models: Cell lines		
Human GB cell lines LN229	ATCC	Cat#CRL-2611
Human GB cell lines U87	ATCC	Cat#HTB-14
Human GB cell lines U118	ATCC	Cat#HTB-15
Experimental models: Organisms/strains		
Mouse: CAnN.Cg-*Foxn1*^{nu}/CrlVr (BALB/c Nude)	Charles River	N/A
Oligonucleotides		
siRNA targeting sequence: Smurf1: 5′-GCGUUUGGAUCUAUGCAAATT-3′	This paper	N/A
siRNA targeting sequence: PTEN: 5′-CCACCACAGCUAGAACUUATT-3′′	This paper	N/A
Recombinant DNA		
PCDH-3HA-puro-PTEN	This paper	N/A
pCMV-PTEN	Addgene	Cat#28298
Software and algorithms		
Live Image 4.0 software	Caliper Life Science	https://www.perkinelmer.com.cn/lab-products-and-services/resources/in-vivo-imaging-software-downloads.html?_ga=2.29909951.1041849854.1637318373-1604795059.1637318373

RESOURCE AVAILABILITY

Lead contact

Further information and requests for resources and reagents should be directed to and will be fulfilled by the lead contact, Lei Dong (ldong@bit.edu.cn).

Materials availability

The cell lines and plasmids that were generated in this study will be available upon reasonable request.

Data and code availability

All data that can support the conclusions of this article are included in the article.

MATERIALS AND METHODS

Cell culture

Human GB cell lines LN229, U87, U118 were procured from the ATCC. For cell culture, DMEM was used with added FBS (10%), penicillin (100 U/mL) and streptomycin (100 μg/mL). Cultured cells were incubated at standard growth conditions, 37°C and 5% CO_2.

Plasmids constructs

pCMV-PTEN was obtained from Addgene. pCMV-PTEN was employed to amplify a full-length PTEN cDNA which was then loaded onto PCDH-3HA-puro vector with Gibson assembly method. The plasmid was confirmed by sequence analysis.

Primary cell culture

Fresh tissue from patients was stored in dry ice during transportation. The tissues were cut into small pieces and washed thrice with 1 × PBS added with antibiotics penicillin (100 U/mL) and streptomycin (100 μg/mL). Next, sample was exposed to EDTA-trypsin at 37°C to digest small tissue pieces. After 10 min of tissue digestion, the suspension was collected, centrifuged, and finally resuspended in fresh medium. Finally, cells were allowed to propagate at 37°C, 5% CO_2.

Stable cell lines

To develop lentivirus, viral particles (psPAX2 packaging and pMD2.G envelope plasmids) with shSmurf1 or PCDH-3HA-puro-Smurf1 and its mutant plasmids were transfected into HEK293T cells. Transfection reagent, lipofectamine 2000 (Invitrogen) was employed as per manufacturer's instructions, and every 6 h post-transfection media was renewed. The supernatant of culture medium containing lentivirus was collected 48 h later. Lastly, exposures of target cells to lentivirus containing supernatant in the presence of polybrene (Solarbio) give rise to stable cell lines. The selection was accomplished by puromycin (2 μg/mL) for 48 h.

RNA interference

Human siRNA against Smurf1 was 5′-GCGUUUGGAUCUAUGCAAATT-3′, and si-PTEN was 5′-CCACCA CAGCUAGAACUUATT-3′. Then cells were transfected with siRNAs using Lipofectamine RNAiMAX reagent (Invitrogen) under the provided protocol. Briefly, siRNAs and Lipofectamine RNAiMAX were incubated with DMEM. After 5 min, mixing/shaking of siRNAs and RNAiMAX was done before the second round of incubation for 15 min at ~25°C. In the end, this mixture was added to cells for 24 h followed by washing with fresh medium. 72 h after transfection, proteins were examined by western blotting.

Clonogenic assay

The impact of treatments on the proliferation of GB cells was assessed via colony-forming capability. Cancer cells (10^3/well) were seeded and grown in three separate 6-well plates. The culture was terminated when the cells formed visible colonies. Cells were washed twice with 1 × PBS, followed by 15 min fixation with methanol. Cells were visualized by 30 min staining with crystal violet (0.1%). Finally, cell colonies were counted and recorded.

Western blotting for protein analysis

Treated and control cells were collected and exposed to RIPA lysis buffer. Separation of the boiled proteins in sample buffer was achieved via SDS-PAGE. Proteins were then transferred to PVDF membranes, which were blocked using 5% nonfat dry milk followed by incubation (4°C) with primary antibodies. After 12 h, the second round of incubation at room temperature was implemented with peroxidase-conjugated secondary antibodies for 1 h. Finally, enhanced chemiluminescence was used to visualize bound antibodies.

Primary antibodies were used as per manufacturer's instructions and standard dilutions: Smurf1 (ab57573, Abcam); Akt and p-Akt Ser473 (#9272 and #4060 respectively, CST); β-actin (A1978-200, Sigma); PTEN (sc-7974, Santa); PTEN (10047-1-AP, Proteintech); PTEN (ABM-2052, Cascade BioScience); EGFR (#4267, CST); Phosphotyrosine (p-4G10) (05-321X, EMD Millipore); HA (M180-3, MBL International); Ki67 (ab15580, Abcam); p-p70S6K Thr389 (#9205, CST); p70S6K (sc-8418, Santa); 4EBP1 (#9644, CST); p-4EBP1(#2855, CST). The following secondary antibodies were used: Goat anti-Rabbit IgG (H+L) (HRP) Polyclonal (PI-31460, Thermo Fisher); Goat anti-Mouse IgG (H+L) (HRP) Polyclonal (PI-31430, Thermo Fisher).

Immunofluorescence

The slides were treated with Xylene and Ethanol, then put into 50 ml Sodium Citrate Buffer (SCB composition: 41 ml 0.1 M sodium citrate + 9 ml 0.1 M critic acid + H_2O to 500 ml); boiled in the microwave oven, and cooled to room temperature. The slides were treated with 3% H_2O_2, then 5 min with 0.2% Triton X-100, and 10% goat serum for 60 min. Subsequently, an overnight incubation of slides with the primary antibody at 4°C followed by 30 min incubation with the secondary antibody (EnVision™+ Dual Link System-HRP) at room temperature. Later, slides were incubated with DAB and Hematoxylin. The involvement of human participants and analysis on the obtained samples were approved by the Ethics Committee of the Beijing Institute of Technology (BIT). Informed written consent was obtained from all the participants. The study methodologies observed all the standards posed by the Declaration of Helsinki.

Flow cytometry analysis

For detection of the cell cycle, the indicated treated cells were collected and fixed with 70% ethyl alcohol for 12 h at 4°C followed by staining with propidium iodide (PI). Flow cytometry was then employed to identify stained cells. Annexin V-FITC/PI apoptosis detection kit was used to analyze apoptotic cells. In brief, 5×10^5 cells of each group were harvested by trypsinization after treatment with Torin1, ShSmurf1, and Torin1+ShSmurf1 for 24 h. Next, PBS and binding buffer (50 uL) were used to wash and resuspend the cells, respectively. Then 5 uL of each, Annexin V-FITC and PI, were added to the cell suspensions and incubated in the dark at room temperature for 10 min. Finally, the samples were evaluated by flow cytometry (BD Aria III), and FlowJo 7.6 software was used to analyze the data.

Bioluminescence imaging and reporter gene assay based *in vivo* screening

We deliberately introduced a CMV promoter-luciferase reporter in LN229 cells through G418 selection. To measure Firefly Luciferase activities, a Dual Luciferase® Reporter (DLR™) Assay System was employed. LN229-CMV-Luc cells were then transfected with shSmurf1 or shPLKO. Bioluminescence imaging (BLI) was carried out ahead of treatment with the IVIS® Spectrum *in vivo* imaging system (PerkinElmer). Ten minutes before imaging, D-luciferin (Promega Cat#1041) was administered intraperitoneally into the animals (64 mg/kg). Isoflurane was used to keep animals anesthetized while imaging. Live Image 4.0 software was used to quantify the signal intensity. The animal study was approved by the Animal Protection and Ethics Committee of BIT. All experiments were conducted according to the animal protection rules prescribed by the said committee.

EXPERIMENT MODEL AND SUBJECT DETAILS

Mouse models

All protocols and procedures were also approved by the BIT's Animals Care and Use Committee. For flank tumor implantation, mice were comforted and injected in the back with a syringe. The procedure is considered non-harmful and with little pain. For intracranial tumor implantation, 10-12 weeks old female athymic nude mice (Charles River) were used. To induce unconsciousness, a mixture (2:1) of ketamine (100 mg/kg) and xylazine (10 mg/kg) was injected intraperitoneally. Local anesthesia (procaine) was also applied at the incision site. A stereotaxic frame was employed to immobilize the anesthetized animals. Then, using 24G Hamilton syringe, 3 mm intracranial injections were performed to introduce 1×10^6 GB cells (injection

coordinates: 2 mm anterior, 1.5 mm lateral to the brain's right hemisphere relative to bregma). Bioluminescence imaging was performed under anesthesia (sevoflurane) and caused no pain to the animals. Mice were observed post-inoculation to ensure activity and food intake. The ending point (weight loss greater than 20%, hunched, etc.) was set to ensure that the animals were suffering no pain.

QUANTIFICATION AND STATISTICAL ANALYSIS SECTION

All experiments were repeated two to three times with the indicated numbers of cells or mice. Data are presented as mean ± SD. Statistical significance was determined unpaired two-tailed Student's *t*-test. For imaging analyses, two-tier tests were used to first combine technical replicates and then evaluate biological replicates. *$p < 0.05$; **$p < 0.01$; ***$p < 0.001$; NS, not significant.